Stellar Populations of Bulges of Disc Galaxies in Clusters

Lorenzo Morelli[1,5]
Emanuela Pompei[2]
Alessandro Pizzella[1]
Jairo Méndez-Abreu[1,3]
Enrico Maria Corsini[1]
Lodovico Coccato[4]
Roberto Saglia[4]
Marc Sarzi[6]
Francesco Bertola[1]

[1] Dipartimento di Astronomia, Università di Padova, Italy
[2] ESO
[3] INAF-Osservatorio Astronomico di Padova, Italy
[4] Max-Planck-Institut für Extraterrestrische Physik, Garching, Germany
[5] Department of Astronomy, Pontificia Universidad Católica de Chile, Santiago, Chile
[6] Centre for Astrophysics Research, University of Hertfordshire, Hatfield, United Kingdom

Photometry and long-slit spectroscopy are presented for 14 S0 and spiral galaxies of the Fornax, Eridanus and Pegasus clusters and the NGC 7582 group. The age, metallicity and α/Fe enhancement of the stellar population in the centres and their gradients are obtained using stellar population models with variable element abundance ratios. Most of the sample bulges display solar α/Fe enhancement, no gradient in age, and a negative gradient of metallicity. One of the bulges, that of NGC 1292, is a pseudobulge and the properties of its stellar population are consistent with a slow build-up within a scenario of secular evolution.

The relative importance of dissipative collapse (Gilmore & Wyse, 1998), major and minor merging events (Aguerri, Balcells & Peletier, 2001), and redistribution of disc material due to the presence of a bar or environmental effects (Kormendy & Kennicutt, 2004) drives the variety of observed properties in bulges. The bulges of lenticulars and early-type spirals are similar to low-luminosity elliptical galaxies and their photometric and kinematic properties satisfy the same fundamental plane (FP) correlation found for ellipticals. The surface-brightness radial profile of large bulges is well described by the de Vaucouleurs law, although this law can be drastically changed taking into account the small-scale inner structures, smoothed by the seeing in ground-based observations. Some bulges are rotationally-flattened oblate spheroids with little or no anisotropy. But, the intrinsic shape of a large fraction of early-type bulges is triaxial, as shown by the isophotal misalignment with respect to their host discs and non-circular gas motions. The bulk of their stellar population formed between redshifts 3 and 5 (~ 12 Gyr ago) over a short timescale. The enrichment of the interstellar medium is strongly related to the time delay between type II and type Ia supernovae, which contributed most of the α elements and iron, respectively.

On the contrary, the bulges of late-type spiral galaxies are reminiscent of discs. They are flat components with exponential surface brightness radial profiles and rotate as fast as discs. Moreover, the stellar population in late-type bulges is younger than in early-type bulges. They appear to have lower metallicity and lower α/Fe enhancement with respect to early-type galaxies.

In the current paradigm, early-type bulges were formed by rapid collapse and merging events, while late-type bulges have been slowly assembled by internal and environmental secular processes (Kormendy & Kennicutt, 2004). But many questions are still open. For instance, the monolithic collapse scenario cannot explain the presence in bulges of kinematically-decoupled components. Moreover, the environment plays a role in defining the properties of galaxies. Recent studies of early-type galaxies in different environments have shown that age, metallicity, and α/Fe enhancement are more correlated with the total mass of the galaxy than local environment.

To investigate the formation and evolution of bulges, there are two possible approaches: going back in redshift and looking at the evolution of galaxies through cosmic time; or analysing nearby galaxies in detail to understand the properties of their stellar population in terms of the dominant mechanism at the epochs of star formation and mass assembly. We present a photometric and spectroscopic study of the bulge-dominated region of a sample of spiral galaxies in clusters. Our aim is to estimate the age and metallicity of the stellar population and the efficiency and timescale of the last episode of star formation in order to disentangle early rapid assembly from late slow growth of bulges.

Sample, photometry, and spectroscopy

In order to simplify the interpretation of the results, we selected a sample of disc galaxies, which do not show any morphological signature of having undergone a recent interaction event. All the observed galaxies are classified as non-barred or weakly barred galaxies. They are bright ($B_T \leq 13.5$) and nearby (D < 50 Mpc) lenticulars and spirals with a low-to-intermediate inclination ($i \leq 65°$). Twelve of them were identified as members of the Fornax, Eridanus and Pegasus clusters and a further two are members of the NGC 7582 group.

The photometric and spectroscopic observations of the sample galaxies were carried out in three runs at ESO La Silla in 2002 (run 1), 2003 (run 2) and 2005 (run 3). We imaged the galaxies with the Bessel R-band filter. In runs 1 and 2 spectra were taken at the 3.6-m telescope with EFOSC2; in run 3 spectra were obtained with EMMI on the NTT in red medium-dispersion mode.

In order to derive the photometric parameters of the bulge and disc, we fitted iteratively a model of the surface brightness to the pixels of the galaxy image using a non-linear least-squares minimisation. We adopted the technique for photometric decomposition developed in GASP2D by Méndez-Abreu et al. (2008, see Figure 1). We measured the stellar kinematics from the galaxy absorption features present in the wavelength range and centred on the Mg line triplet at 5 200 Å by applying the Fourier correlation quotient method (Bender et al., 1994). We also measured the Mg, Fe, and H_β line-strength indices from the flux-calibrated spectra. We indicate the average iron index with <Fe> = (Fe5270 + Fe5335)/2, and the magnesium-iron index with [MgFe]' = Mg_b (0.72 × Fe5270 + 0.28 × Fe5335) (see Fig-
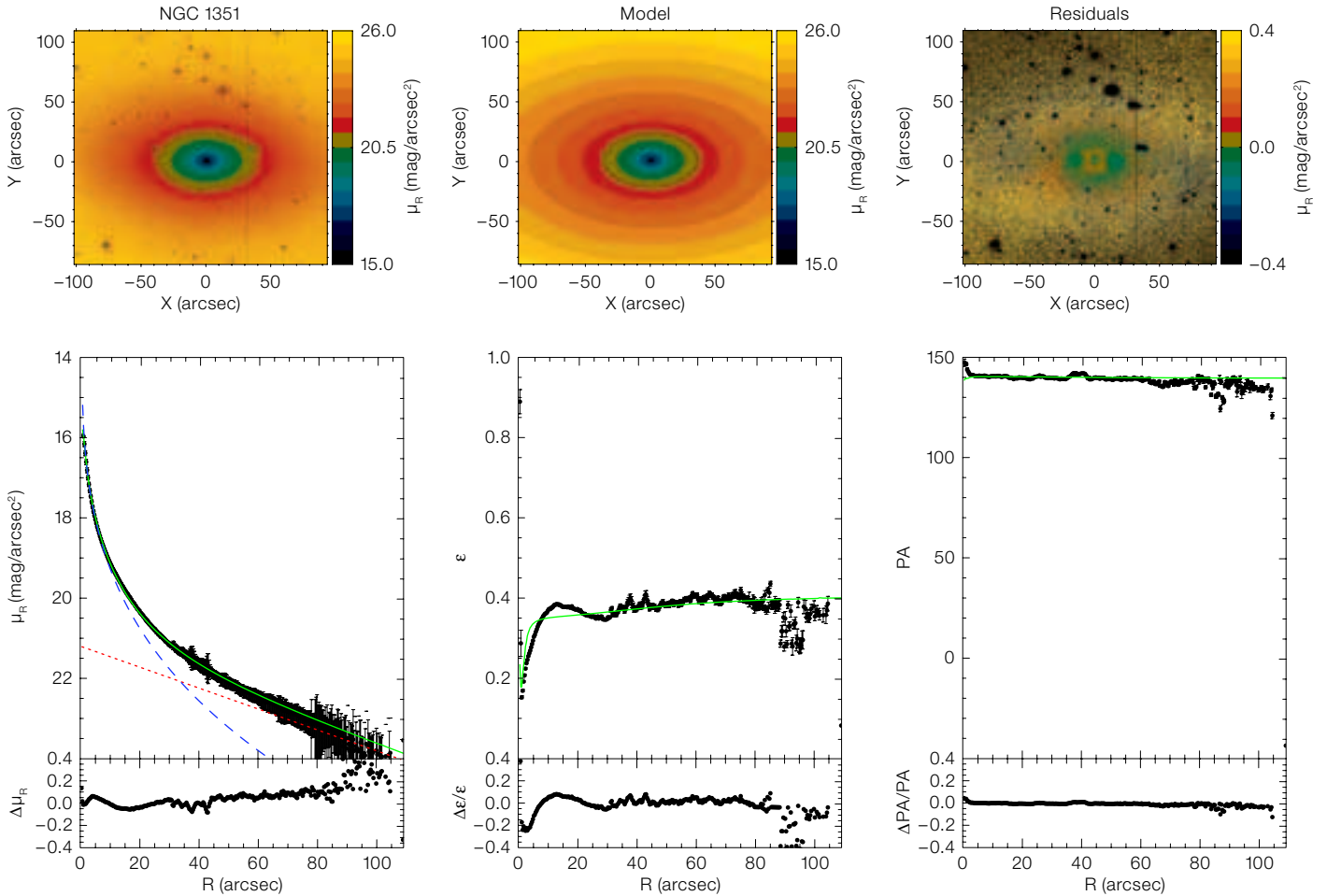
Figure 1 (above). Two-dimensional photometric decomposition of a sample galaxy, NGC 1351. **Upper panels (from left to right):** Map of the observed, modelled and residual (observed-modelled) surface-brightness distribution of the galaxy. **Lower panels (from left to right):** Ellipse-averaged radial profile of surface-brightness, position angle, and ellipticity measured in the observed (dots with error-bars) and modelled image (solid line). Residuals on the observed model are shown in the bottom plots.

ure 2). The H_β line-strength index was measured from the resulting H_β absorption line, after the emission line was subtracted from the observed spectrum.

Age, metallicity, and α/Fe enhancement: central values

From the central line-strength indices we derived the mean ages, total metallicities and total α/Fe enhancements of the stellar populations in the centre of the
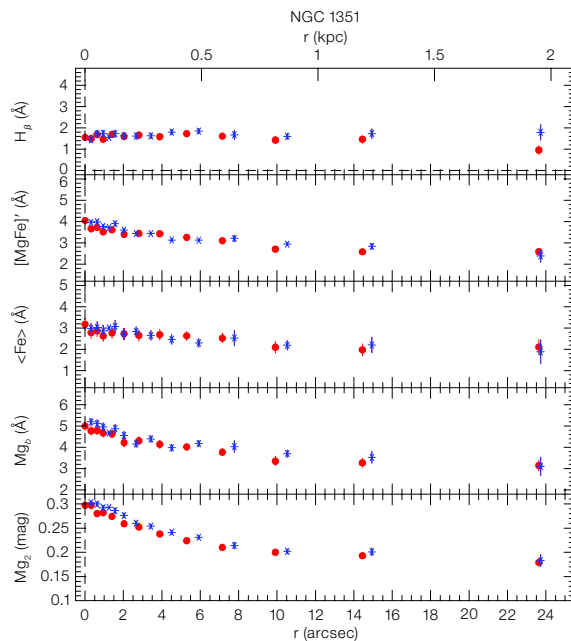
Figure 2. The line-strength indices measured along the major axes of one of the sample galaxies, NGC 1351. **From top to bottom:** East-west folded radial profiles of H_β, [MgFe]′, <Fe>, Mg_b, and Mg_2. Asterisks and dots refer to the two sides (east/west) of the galaxy.
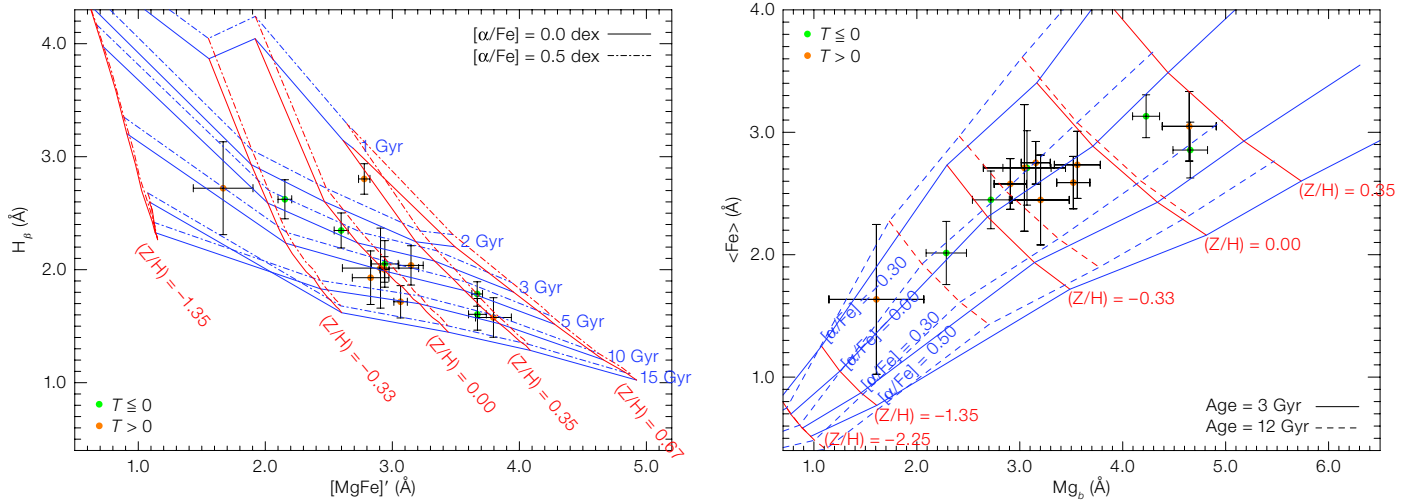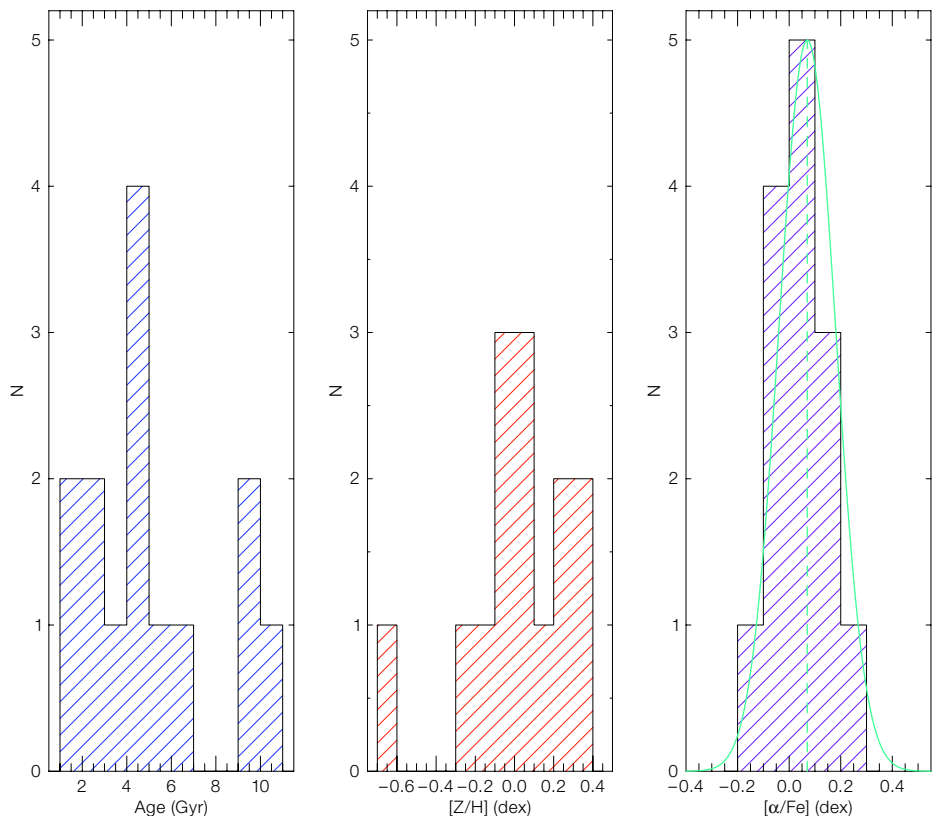
Figure 3 (above). The distribution of the central values of H_β and [MgFe]' indices (left panel) and <Fe> and Mg_b indices (right panel) averaged over 0.3 r_e for the 15 sample galaxies. Points are coloured according to their RC3 galaxy type. The lines indicate the models by Thomas et al. (2003). **Left panel:** The age–metallicity grids are plotted with two different α/Fe enhancements: [α/Fe] = 0.0 dex (continuous lines) and [α/Fe] = 0.5 dex (dashed lines). **Right panel:** The [α/Fe]–metallicity grids are plotted with two different ages: 3 Gyr (continuous lines) and 12 Gyr (dashed lines).

sample bulges by using the stellar population models of Thomas et al. (2003) shown in Figure 3. These models predict the values of the line-strength indices for a single stellar population as function of the age, metallicity, and [α/Fe] ratios.

Three classes of objects were identified, according to their age and metallicity (Figure 4). The young bulges are scattered about an average age of 2 Gyr with hints of star formation, as shown by the presence of the H_β emission line in their spectra. The intermediate-age bulges span the age range between 4 and 8 Gyr. They are characterised by solar metallicity. Finally, the old bulges have high metallicity and a narrow distribution in age around 10 Gyr.

Although the correlations are not statistically very strong, the elliptical and S0 galaxies ($T < 0$, where T is the numerical RC3 galaxy type) have bulges older and more metal-rich than the spirals ($T > 0$) in the central region. Most of the sample bulges display solar α/Fe enhancements with the median of the distribution at [α/Fe] = 0.07 dex (Figure 4, right panel).
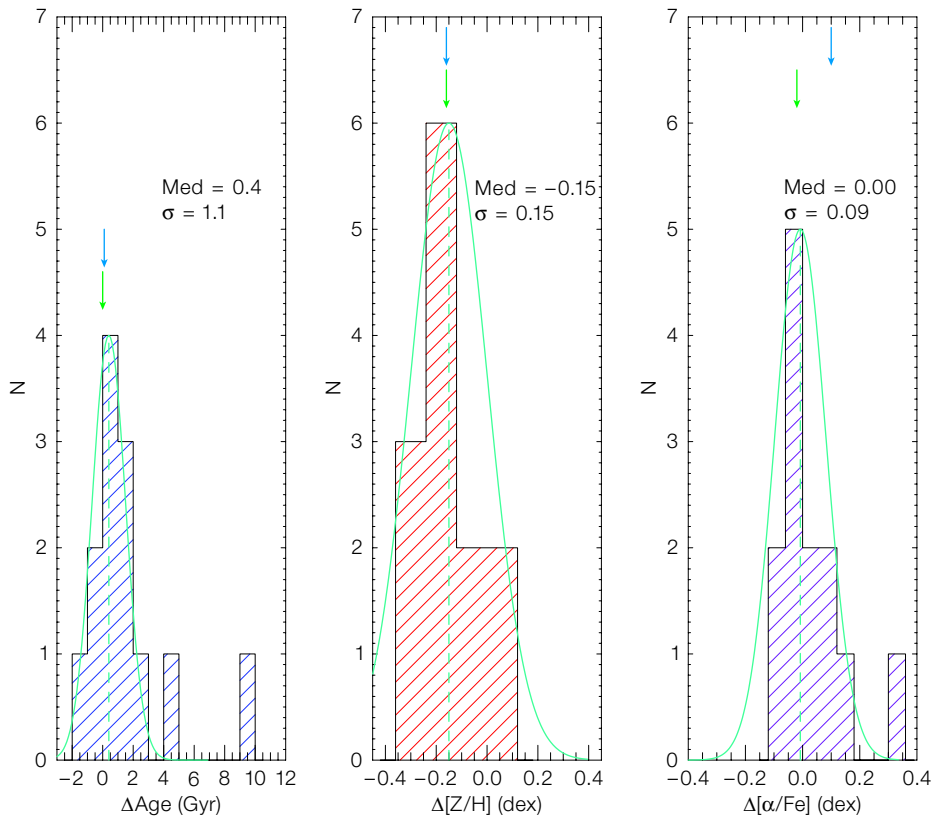

Figure 4. Distribution of age (left panel), metallicity (central panel) and α/Fe enhancement (right panel) for the central regions of the sample galaxies. The solid line in the right panel represents a Gaussian centred at the median value [α/Fe] = 0.07 dex of the distribution. Its width, σ = 0.11, is approximated by the value containing 68 per cent of the objects of the distribution.

Age is mildly correlated with velocity dispersion, and α/Fe enhancement. We conclude that the more massive bulges of our sample galaxies are older, more metal-rich and characterised by rapid star formation.

Age, metallicity and α/Fe enhancement: gradients

Different formation scenarios predict different radial trends of age, metallicity, and α/Fe enhancement. Therefore the radial gradients of the properties of the stellar populations of bulges are a key piece of information to understand the processes of their formation and evolution. In the monolithic collapse scenario, gas dissipation towards the galaxy centre, with subsequent occurrence of star formation and galactic winds, produce a steep metallicity gradient. A strong gradient in α/Fe enhancement is expected too. The predictions for bulges forming through long time-scale processes, such as dissipationless secular evolution, are more contradictory. In the latter scenario the bulge is formed by redistribution of disc stars. The gradients possibly present in the progenitor disc could be either amplified, since the resulting bulge has a smaller scalelength than the progenitor, or erased as a consequence of disc heating (Moorthy & Holtzman, 2006).

An issue in measuring the gradients of age, metallicity, and [α/Fe] in bulges could be the contamination of their stellar population by the light coming from the underlying disc stellar component. This effect is negligible in the galaxy centre but it could increase going to the outer regions of the bulge, where the light starts to be dominated by the disc component. In order to reduce the impact of disc contamination and extend as much as possible the region in which gradients were derived, we mapped them inside r_{bd}, the radius where the bulge and disc give the same contribution to the total surface brightness. For each galaxy, we derived the Mg_2, H_β, and <Fe> line-strength indices at the radius r_{bd}. The gradients were set as the difference between the values at centre and r_{bd}, and their corresponding errors were calculated through Monte Carlo simulations. The indices were converted into gradients

Figure 5. Distribution of the gradients of age (left panel), metallicity (central panel) and α/Fe enhancement (right panel) within radius r_{bd} at which bulge and disc give equal brightness contributions for the sample galaxies. Dashed line represents the median of the distribution and its value is listed. Solid line represents a Gaussian centred at the median value of the distribution. The width of the distributions, σ, are approximated by the value containing 68 per cent of the objects and are also listed. The green and blue arrows show the average gradient found for early-type galaxies and bulges by Mehlert et al. (2003) and Jablonka et al. (2007), respectively.

of age, metallicity, and α/Fe enhancement following Thomas et al. (2003) and are shown in Figure 5.

Most of the sample galaxies show no gradient in age with the median of the distribution at 0.4 Gyr. Negative gradients of metallicity were observed and the number distribution shows a clear peak at [Z/H] = −0.15 dex. The presence of a negative gradient in the metallicity radial profile favours a scenario with bulge formation via dissipative collapse. Dissipative collapse implies strong inside-out formation that should give rise to a negative gradient in the α/Fe enhancement too. But no gradient was measured in the [α/Fe] radial profiles for almost all the galaxies. All the deviations from the median values of the other objects can be explained by their errors alone. No correlation is found between the central value

and gradient of α/Fe enhancement, while the central value and gradient of metallicity are correlated. All these hints suggest that a pure dissipative collapse is not able to explain formation of bulges and that other phenomena like mergers or acquisition events need to be invoked.

Pseudo-bulges

Classical bulges are similar to low-luminosity ellipticals and are thought to be formed by mergers and rapid collapse. Pseudo-bulges are disc or bar components which were slowly assembled by acquired material, efficiently transferred to the galaxy centre where it formed stars. Pseudo-bulges can be identified according to their morphological, photometric, and kinematic properties following the list of characteristics compiled by
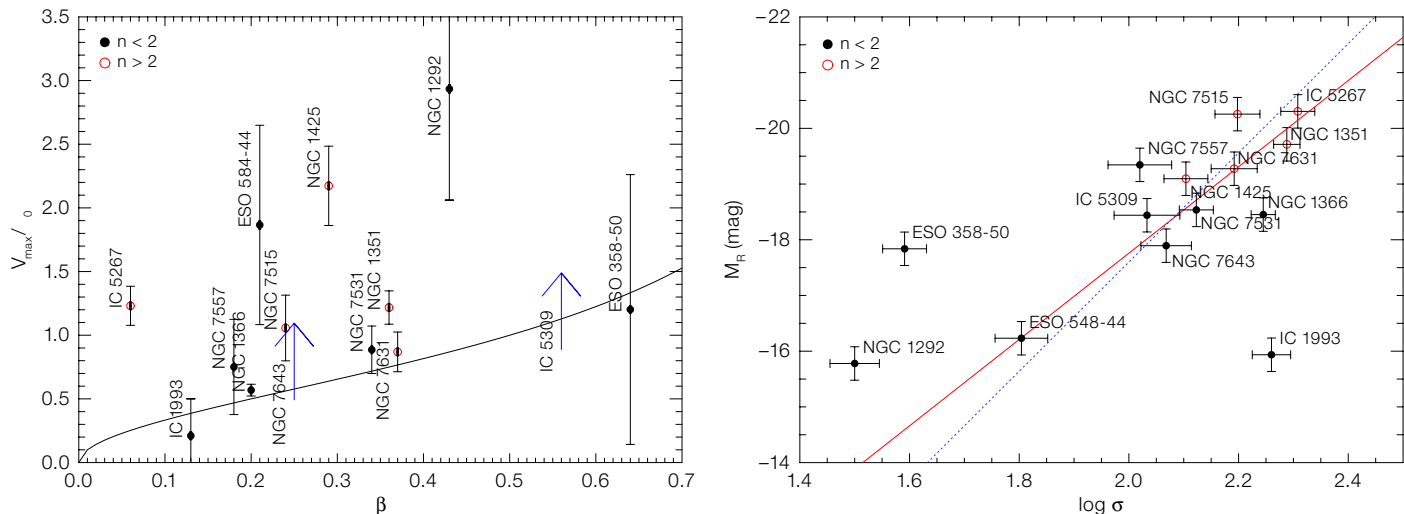
Figure 6. The location (left panel) of the sample bulges in the (V_{max}/σ_0, ε) plane. Filled and open circles correspond to bulges with Sèrsic index $n \leq 2$ and $n > 2$, respectively. The continuous line corresponds to oblate-spheroidal systems that have isotropic velocity dispersions and that are flattened only by rotation. The location (right panel) of the sample bulges with respect to the Faber-Jackson relation by Forbes & Ponman (1999, blue dashed line). Filled and open circles correspond to bulges with Sèrsic index $n \leq 2$ and $n > 2$, respectively and the linear fit is shown (red continuous line).

Kormendy & Kennicutt (2004). The more characteristics applied, the safer the classification becomes. Pseudo-bulges are expected to be more rotation-dominated than classical bulges, which are more rotation-dominated than giant elliptical galaxies. We measured the maximum rotation velocity V_{max} within r_{bd} from the stellar velocity curve and the central velocity dispersion σ_0 from the velocity dispersion profile. For each galaxy we derived the ratio V_{max}/σ_0. In Figure 6 (left panel) we compare it to the value predicted for an oblate spheroid with an isotropic velocity dispersion and the same observed ellipticity (Binney & Tremaine, 1987).

Another defining characteristic of pseudo bulges are their position on the Faber-Jackson relation. The pseudo-bulges fall above the Faber-Jackson correlation between the luminosity of the elliptical galaxies and early-type bulges and their central velocity dispersion (Kormendy & Kennicutt, 2004). Sample bulges, except for ESO 358-50 and NGC 1292, are consistent with the R-band Faber-Jackson relation we built from Forbes & Ponman (1999, $L \propto \sigma^{3.92}$). They are characterised by a lower velocity dispersion,

or equivalently a higher luminosity, with respect to their early-type counterparts (Figure 6, right panel). According to the prescriptions by Kormendy & Kennicutt (2004), the bulge of NGC 1292 is the most reliable pseudo-bulge in our sample. Information about its stellar population gives more constraints on its nature and formation process. In fact, the NGC 1292 bulge population has an intermediate age and low metal content. The α/Fe enhancement is the lowest in our sample suggesting a prolonged star-formation history. The presence of emission lines in the spectrum shows that star formation is still ongoing. These properties are consistent with a slow build-up of the bulge of NGC 1292 within a scenario of secular evolution.

References

Aguerri, J. A. L., Balcells, M. & Peletier, R. F. 2001, A&A, 367, 428
Bender, R., Saglia, R. P. & Gerhard, O. E. 1994, MNRAS, 269, 785
Binney, J. & Tremaine, S. 1987, *Galactic Dynamics*, (Princeton, New Jersey: Princeton University Press), 747
Forbes, D. A. & Ponman, T. J. 1999, MNRAS, 309, 623
Gilmore, G. & Wyse, R. F. G. 1998, AJ, 116, 748
Jablonka, P., Gorgas, J. & Goudfrooij, P. 2007, A&A, 474, 763
Kormendy, J. & Kennicutt, R. C. 2004, ARA&A, 42, 603
Mehlert, D., et al. 2003, A&A, 407, 423
Méndez-Abreu, J., et al. 2008, A&A, 478, 353
Moorthy, B. K. & Holtzman, J. A. 2006, MNRAS, 371, 583
Thomas, D., Maraston, C. & Bender, R. 2003, MNRAS, 339, 897